Results in Chemistry 6 (2023) 101181

Contents lists available at ScienceDirect

Results in Chemistry

journal homepage: www.sciencedirect.com/journal/results-in-chemistry

Electro-determination of protonation by tungsten anchored carbon nanoparticle on interdigitated gold electrode

Hanna Ilyani Zulhaimi [a], Subash C.B. Gopinath [a,b,c,d,*], Farizul Hafiz Kasim [a,e], Periasamy Anbu [f]

[a] Faculty of Chemical Engineering & Technology, Universiti Malaysia Perlis (UniMAP), 02600 Arau, Perlis, Malaysia.
[b] Institute of Nano Electronic Engineering, Universiti Malaysia Perlis (UniMAP), 01000 Kangar, Perlis, Malaysia.
[c] Micro System Technology, Centre of Excellence (CoE), Universiti Malaysia Perlis (UniMAP), Pauh Campus, 02600 Arau, Perlis, Malaysia.
[d] Department of Computer Science and Engineering, Faculty of Science and Information Technology, Daffodil International University, Daffodil Smart City, Birulia, Savar, Dhaka 1216, Bangladesh
[e] Centre of Excellence for Biomass Utilization (CoEBU), Universiti Malaysia Perlis (UniMAP), 02600 Arau, Perlis, Malaysia.
[f] Department of Biological Engineering, College of Engineering, Inha University, Incheon 402-751, Republic of Korea.

ARTICLE INFO

Keywords:
Nanomaterial
Electric analysis
Electrolytes
Dielectrode
Current-volt

ABSTRACT

This study presented an enhanced sensitivity of sensing protons (H^+) by anchoring tungsten to carbon nanoparticles (WCN) to encourage high current density on the surface of gold interdigitated electrode (AuIDE). The morphology of the sensor evidences the intactness of electrode surface and suitable for WCN modification. To elucidate the study, unmodified AuIDE was compared to the WCN modified surface. Current-volt analysis was compared with electrolyte scouting in the variation of pH by using a picoammater, which supplied 0.0 to 2.0 V with a 0.1 V ramp interval. It was shown that modified WCN gave the sensitivity in the acidic medium (protons) at the pH 4 with a current density value of 2.5×10^{-5} ampere and increased further with lowering the pH to more acidic. This is due to the fact that the tungsten carbon nanoparticle that is anchored offering more electron density and alters the behavior of the chip. Meanwhile, the current density displayed insignificant changes of current density amplification from pH 5 to 12 with the range of 5.91×10^{-9} to 7.36×10^{-8} Ampere. The deposition of WCN on the AuIDE surface chip revealed the successfulness of this nanoparticle in chemically linked with the AuIDE surface and how modified nanoparticle altered the behavior of the sensing element.

Introduction

The recent development of sensors calls-up for application with *in-situ* and rapid analyses, at the same time producing high accuracy, especially in the field of clinical and health monitoring, drug delivery or markers that indicate the disease severity [1]. Intrinsically, design fabrication, the design process of the chip, modification of chip surface, and volume sample are a few of the factors which can be taken into consideration in developing a high degree of chip sensitivity, surface-to-volume ratio, signal response, selectivity, and conductivity [2,3]. Although researchers progressively develop biosensor on such circumstance, there are drawbacks to the newly developed sensor with is yet to have a loophole in tackling the issue [4]. The existing commercial systems are time-consuming and needs a know-how person to operate it. Another key challenge in the development of the sensor is enhancing its performance by increasing the area of the active surface without increasing the geometric surface of the electrode. This eventually will affect electrode recording that gives small impedance to achieve low and high signal-to-noise ratio [5].

Generally, the development of biosensors has varied approaches but with the same goal which is to have high sensitivity and robustness to have better detection, particularly for medical applications [6]. Gold interdigitated electrode (AuIDE) has proven to be among the best candidates as substrate in chip fabrication because of its adaptability. Notionally, gold has been widely known to employ in sensing applications. Its unique characteristics possess excellent behaviour where it can produce a high degree of sensitivity by the fact of having rapid electron transfer for electrical conductivity. Recent work by Mie et al. (2023) can fabricate nanostructured gold film electrodes that derived gold solution with Au, H, and O in plasma processing in the presence of hydrogen peroxide [7]. The preparation shows that the nanostructured formed on its electrode can be directly used via the "drop-and-dry" method without

* Corresponding author at: Faculty of Chemical Engineering & Technology, Universiti Malaysia Perlis (UniMAP), 02600 Arau, Perlis, Malaysia.
E-mail address: subash@unimap.edu.my (S.C.B. Gopinath).

https://doi.org/10.1016/j.rechem.2023.101181
Received 15 September 2023; Accepted 24 October 2023
Available online 27 October 2023

engaging pre-treatment that commonly involve surfactant and reductant compound for its electrochemical application. HER catalytic current was produced 10 times larger than normal gold electrode and its DET in redox enzyme produced a higher electron transfer rate constant with the presence of its potential substrate. The work evidenced that the anticipation of gold is to expect to have better performance as an electrode. Furthermore, the gold electrode has been commonly used in interdigitated electrodes because it can act as a charger separation and collection mechanism that is able to enhance performance. Because of its charge separation nature that mainly contributes to its severe higher reflection caused by the unwanted shadowing effect that will cause low responsivity [8]. Furthermore, gold possesses excellent conjugate agents and is commonly known to be the best candidate to tailor its surface alteration in attempting to conjugate with chemicals or compound to perform sensor functionality. This is due to the reason it will produce high stability and robust thiol surface [9]. With careful preparation and methods, the characterization of the gold electrode can be exploited to fit its pertinent.

Carbon is widely known to be prime material in technological applications because of its great diverse carbon allotropes that include carbon nanoparticles, carbon nanowall, and graphene. It's derivatives and non-noble metal compound have shown to have excellent performance with myriad functionalities and low-cost alternatives. Because carbon is readily available and relatively cheaper compared to other materials, it has dielectric properties which makes it the widest range of application. Eivazzadeh-Keihan et al. [10,11] reviewed the capability of carbon material in biosensing applications and claimed that it has excellent incorporation with other materials that enable them to chemically bind with other substrates. In the case of carbon nanoparticles, their physical appearance that has relatively small size than macro size makes them exhibit a larger surface-to-volume ratio that enhances high conductivity and sensitivity. An elucidation work by Lu et al. [12] on the capability of carbon nanoparticles with target miRNA that has complex biological properties [13]. In the design phase, they successfully developed a cyclic enzymatic amplification method for sensitive detection in miRNA which shows CNPs act as a protective barrier for target-activated enzymatic digestion property. The element of cyclic reaction helps to enhance the fluorescent signal amplification. It is also worth mentioning that the procedure involved was simple with mix-and-measure steps that can complete in less time.

With regards to the exploration of carbon-supported materials such as tungsten carbide, WC has been studied due to its electrochemical stability, superior electronic conductivity, and its great abundant resources. The versatility of WC makes it easy to support materials that include graphitic carbon, carbon nanotube, graphene, carbon fiber, and carbon nanoparticles. Furthermore, the additional tungsten element prevents aggregation from the nanoparticle surface and will attach byproducts from any processes which consequently reduces the conductivity and stability of the catalyst [14]. The high valency of tungsten with six oxidative states indicates that tungsten is capable to bind with up to six molecular compounds. Curran (2022) reviewed the vast variation of tungsten complexes that include cyclic and non-cyclic Pi complexes of tungsten from ligand alkenes, alkynes, alkenes, allyls, cyclobutadienes, cyclopentadienes, pyrrolides, arenes, cycloheptatrienyl, and C_{60} with different types of reactions involved [15]. In other work by Chen et al. (2019), they were successfully fabricating different variations of WC_x/CN products by manipulating their annealing temperature and reaction time [16]. The experimental procedure resumed with alkali treatment to synthesize single atoms. It was shown that controlling its temperature may exploit the tungsten growth from nanocrystals to single atoms with different tungsten-nitrogen-carbon coordination. The experimental work provides an insight that different types of WC-nanocrystals and WC-single atoms exhibit contrary behaviours and carry different capacities and efficacy in their application.

In this regard, previous work demonstrated the incorporation of carbon-supported material can significantly improve the existing limitation on stability performance and accuracy of signal production [17–20]. The main goal of this study is to improve gold-interdigitated electrode surface performance by modifying its electrode surface with carbon nanoparticles. It is, however, will be the key challenge for tungsten carbon nanoparticles to be attached to on interdigitated gold electrode (AuIDE). To affirm its modification successfulness is by studying its behavior from different ways of analyses. Analysis of electrolyte scouting will serve as the assessment of sensitivity and rapid performance of electron transfer. Furthermore, carbon nanoparticles will be responsible to enhance the performance of AuIDE due to its conductivity while tungsten will make a great contribution to the rapid electron transfer for biosensing applications. It is hoped fabrication of nanoparticles onto AuIDE will be the reference to overcome the abovementioned limitations.

Materials and methods

Chemicals

Vulcan Carbon black XC72R was obtained from Fuel Cell Store. Methanol (99.8 %) ACS reagent, Potassium Chloride, (90 %) flakes, and tungsten (IV) hexachloride, ≥99.99 trace metal basis was purchased from Merck, Germany. Deionized water was obtained from a laboratory in the Institute of Nano Electronic Engineering, Universiti Malaysia Perlis. The chip DRP-G-IDEAU10 was purchased from Metrohm, Malaysia. 1,1′-Carbonyldiimidazole (CDI) was purchased from Sigma-Aldrich, USA. The accurate pH solutions from 1 to 12 were purchased from HANNA Instruments, Malaysia. All the chemical reagents used in this study were in analytical reagent grade.

Synthesis of tungsten anchored on carbon nanoparticle (WCN)

Initially, 0.2 mg of Pt/C (20 %) was weighed in the vial. Argon gas was introduced in the vial to remove air and oxygen. Subsequently, ethanol was introduced into the vial with the drop-by-drop method and carefully handled in the presence of argon gas to avoid a spark from the reaction. Once ethanol was successfully suspended in methanol, the vial was then closed and sealed by using parafilm and sonicated for 1 h. Meanwhile, in different vials, tungsten (IV) hexachloride was added to methanol with mol ratio Pt:W = 1, and let it mix using a vortex mixer before it was sonicated for 20 s. Later, the mixture of tungsten (IV) hexachloride and methanol was subsequently discarded to room temperature for 5 min before it was mixed with Pt/C immersed in methanol. Upon the completion of both vials mixed, it was followed by the drying method in a hotplate at 60 Celsius for 1 h at ambient temperature. The sample was then collected and further underwent an annealing process in rapid thermal annealing (RTA) system. The annealing was then preceded to operate at 650 Celsius for 2 h under ammonia gas at 100 sccm with a ramp rate of 100 Celsius/10 min. Before the annealing process took place, the sample was purged with argon gas and later with ammonia gas at ambient temperature. The sample in black powder was discarded from RTA after it cools to ambient temperature. The final sample discarded from the RTA system was then prepared for alkali treatment using potassium hydroxide in 1.5 M for 24 h.

Functionalized AuIDE chip with modified WCN

To perform functionalization of WCN on AuIDE, the electrodes were pre-cleaned thoroughly with a great amount of deionized water. The electrode was dried by using air blow and it was placed inside the electrode probe station. Next, 20 μL of KOH was dropped on the electrode and let it incubate for 10 min. The subsequent step was to allow the electrode to undergo a cleaning procedure. In the cleaning procedure, the electrode was poured with 10 volumes of deionized water that eventually removed the surface liquid in a manner and removed the remaining by using an air blower. The cleaning procedure was done in

three washings. The next step was applied by dropping 20 μL of 1,1′-Carbonyldiimidazole (CDI) onto the electrode surface that acts as the linker. The electrode was set aside for one hour and it was carefully monitored to ensure no drop of CDI is dried throughout the procedure. Later, it was performed with a cleaning procedure by using deionized water in the abovementioned step. Succeeding to the cleaning procedure, 20 μL of suspended WCN was dropped on the electrode and let it stay onto the electrode for one hour with precaution to avoid the electrode from getting dry. The cleaning procedure was applied to proceed with the steps in electrolyte scouting.

Electrical and electrochemical analysis

The electrical analysis was carried out by using electrolyte scouting. pH scouting was performed in the range of pH 1–12 and it was measured by using a Picoammeter power supply (Keithley 6487). Picoammeter is set to record the measurement in current–potential supply within the range 0 to 2.0 V at 0.1 V each ramp step and the output signal was generated in Volt. Initially, the chip was immersed in a great amount of deionized water and air-blowed the small droplet by using an air blower. Once it was dried, the chip was placed on a probe station. The positive and negative electrodes were placed on an electrode holder that was connected to the positive and negative power supplies with needles. 20 μL of pH 1 was dropped in the sensing region of the electrode, followed by recording the current generated in the picoammeter. Once the volt is completely recorded, a drop of pH 1 was discarded and it was cleaned by using deionized water. The remaining droplets of deionized water was blow dried. This cleaning procedure was performed three times. Next, the procedure for pH 2 until pH 12 was applied in the same approach. All experimental works were carried out in ambient conditions. Fabrication and testing system has been routinely used for point-of-care analysis and found to be environmental stable.

Results and discussion

This study shows the set of data gathered in the experimental works and explains the results obtained. Initially, the result represented on the morphology of the AuIDE chip, furthermore, the mechanism of electrolyte scouting was well discussed, and how its behavior in the electrolyte interrelates with surface modification WCN. The result also gives insight into applications that can be used on the modified WCN. This study highlights one of the applications on the WCN surface in evaluating the occurrence of proton (H +) with electrolyte solutions. The basic abundance of ions in the electrolyte solutions at different pH levels was elucidated and they can move between the electrodes (Fig. 1).

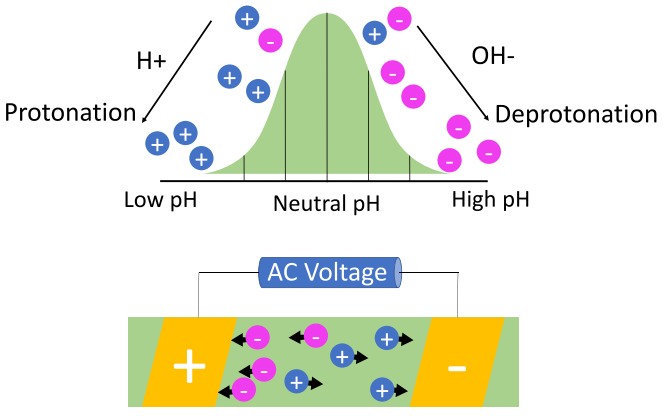

Fig. 1. (a) Illustration on charges with pH ranges. Protonation and deprotonation change with pH ranges are indicated. (b) movement of ions between electrodes.

Surface characterization of WCN-AuIDE

The morphological characteristic of modified WCN functionalization was done to assess its morphological characteristic on the AuIDE surface electrode. Initially, the prepared WCN was observed under FESEM and FETEM set-ups. Both nanoscale imaging observations have revealed the uniformly shaped nanosized particles in (Fig. 2a-c). SEM images reveals the shape of particle is in sphere that reflect to carbon nanoparticle used with average 50 nm size. Further EDX analysis in Fig. 2c clearly indicated that the percentage carbon element has ~ 82 % in the prepared material. The value of percentage weight and atom also shows that carbon element is relatively high in comparison to tungsten element with 0.69 % atom that made it clear on probability of adjacent of tungsten embedded on carbon nanoparticle. FESEM and FETEM images made it clear that modification of WCN does not gives different structure in nanoparticle. Despite that, careful inspection on FETEM images gives evident the presence of small dark dots in which it scattered and overlapped with nanostructure. Interestingly, small dots were happened to position on nanostructure only and it does not disperse independently, of which it could establish the anchoring of tungsten atom on carbon nanoparticle. Nevertheless, the size of tungsten atom cannot be identified due restriction to capture with size below (<1 nm). Initially, tungsten chloride dissolves in methanol that gives end-product of tungsten alkoxides [21]. Tungsten alkoxides acts as precursor is then mixed with defective graphene in carbon nanoparticle to form tungsten carbide nanoparticle. The catalyst precursor and carbon nanoparticle are then mixed, collected, and dried at 60 Celsius. The sample undergone pyrolysis that is above of crystallization temperature. At this temperature, atom migrates and relocates onto the defects of carbon nanoparticle. As it cools back, atom will slowly recrystallize organically to ensure no additional factors were forced during crystallization process. The presence of tungsten atom helps to stabilize the bond that helps to prevent atom from agglomeration during annealing and additional of loading tungsten alters the intrinsic characteristics of carbon nanoparticle. According to Wang et al, cooling down from pyrolysis, vacancy of tungsten atom involves in altering the disorder of graphene matrix of carbon nanoparticle, which can be justified from Raman spectra that gives improved result with additional of tungsten that expands D and G band that also increase I_D/I_G, that benefits on improving its electronic conductivity [22]. Fig. 3 illustrates how tungsten catalyst precursor vacates onto surface of graphite to form tungsten carbide nanoparticle.

3D profiler analysis in Fig. 4a provides 2D image of surface modified WCN on the AuIDE electrode. Positive and negative terminals were on the side region of the chip and where they placed oppositely to each other. It can be shown in Fig. 4a that one of the images based on its physical appearance is a commercialized electrode and they have uniform pattern with scanned image (Fig. 4b). While Fig. 4c showed the image of the sensing surface (AuIDE) under high-power microscope. To further evaluate the fabrication technique implemented, 3D nanoprofiler analysis displayed the color contrast in the AuIDE surface. The red color in Fig. 4d reflects the outer layer formed on AuIDE that is mainly contributed by the chemical bind of modified WCN by using CDI linker. Also, Fig. 4d reveals the formation of green and yellow colors that were underneath the red contrast layer, which mainly comes from its substrate layer, AuIDE. Besides, the surface roughness of red contrast in has shown to have a smooth surface of modified WCN onto the layer form of substrate. This proves the method in binding with substrate has proven to be a success due to its uniformity layer formed by applying chemical linkers.

Surface infrastructure

Fig. 4b depicts the gap of each electrode finger and thickness on the surface of AuIDE. The thickness formed by modified WCN was shown to be between 220 and 256 nm with maximum height being 256.1 nm and it displayed modified WCN surface layers in the uniform surface on each

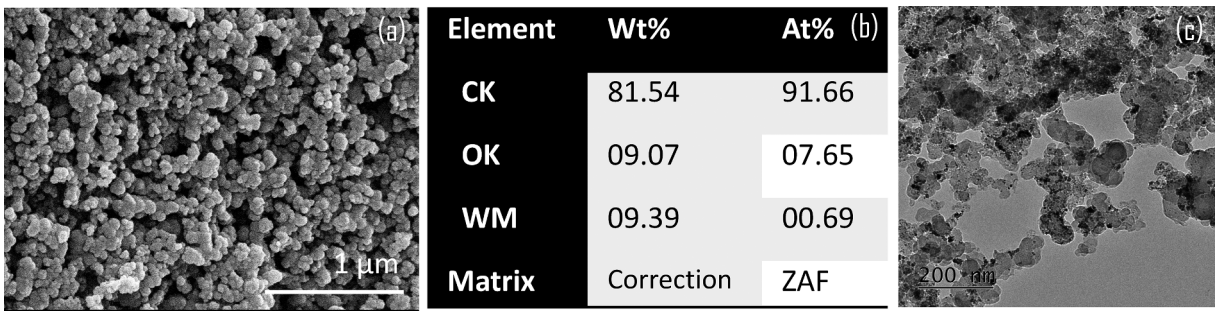

Fig. 2. High-resolution images of the synthesized tungsten-anchored carbon nanoparticle. (a) FESEM image; (b) EDX on FESEM image; (c) FETEM image.

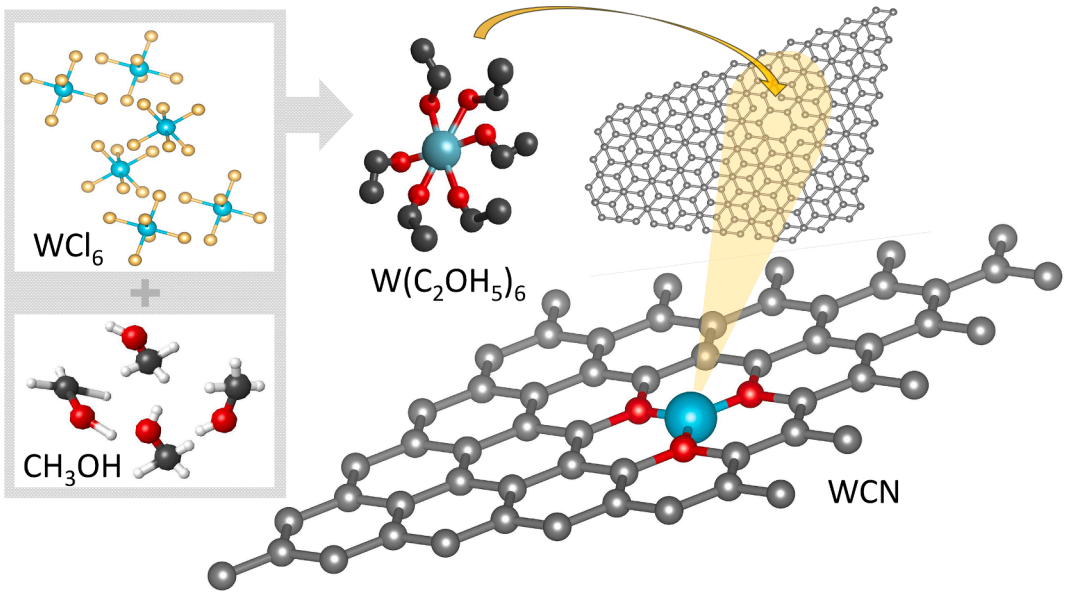

Fig. 3. Schematic diagram for possible reaction pathway of tungsten alkoxide as catalyst precursor for surface layer modification of carbon nanoparticle.

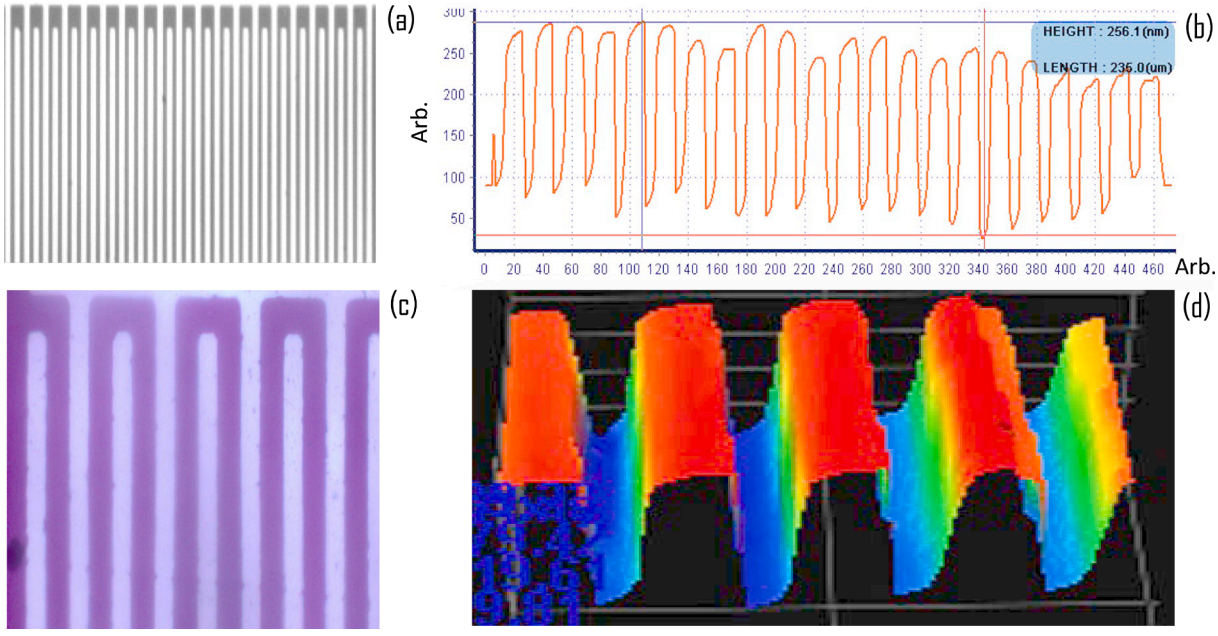

Fig. 4. Images on AuIDE chip. (a) High-Profiler Microscopy image as 2D; (b) surface profile with interlock fingers of AuIDE. (c) High-power microscopy image; (d) 3D-nano profiler image.

finger. This uniformity was achieved by taking precautions while depositing modified WCN while maintaining steps to be applied accordingly. For instance, while dropping KOH and CDI solution onto the AuIDE chip, it was carefully monitored to ensure the solution will not get dry from the evaporation process. The dropping chemicals onto the surface AuIDE procedure took 1 h to ensure the solution is strongly attached to the AuIDE electrode surface. Furthermore, each addition of KOH and CDI solution will undergo a cleaning procedure three times to ensure there is no drop of chemicals that sit on top of the electrode surface and to avoid chemicals getting reacted which consequently will produce unwanted by-products. It has been done in a clean room laboratory. This is to ensure minimal traces that will take effect while fabricating it. This in turn is affected by its surface uniformity. Uniformity surface layer during fabrication is to bind it to ensure having strongly attached to the chip to avoid instability performance of response upon implementation. In addition, rough surfaces may have the potential of misleading value in data reading. It was due to the reason unevenness layer from the fabrication process may affect to ion field pattern during association dissociation, which consequently disrupts ion dissociation [23]. Furthermore, the uneven ion field pattern will have a high possibility to obtain data instability while taking the measurement. The 3D-profilometry analysis provided sufficient evidence that the procedure applied creates a layer of modified WCN. In this study, the formation layer of modified WCN is illustrated in Fig. 4a-d, which gives sufficient evidence of the red contrast of modified WCN deposited onto AuIDE that was fully deposited on the whole surface of the substrate. In addition, the deposition layer formed provides evidence of the success of the CDI solution to be one of the prospective linkers on AUIDE.

Electrical characterization of modified WCN fabrication on AuIDE: Mobile electron potential

The attainment for modified WCN to bind onto AuIDE can also be proved by the electrical curve of current potential in Fig. 5a and 5b, that in general, produced variation current generated in comparison to bare AuIDE. This implies that the CDI solution has the capability to be a multi-ionic linker to bind with many ionic sites of modified WCN that helps to chemically bind with modified WCN, hence increasing its electrical potential. The electrochemical analysis depicts one of the crucial parts of electrochemistry where it involves electrochemical techniques for sensitive detection or monitoring species of target compounds. Theoretically, in electrochemical analysis, chemical reaction aids electrons to move between the electrode in an electrochemical cell containing an analyte. It involves giving up and receiving ions, and where ions are freely to move in between atoms of the compound. Since the electrode is adjacent to opposite sides, the movement of the ions will create a dipole moment [24]. Electron activity was measured in a product of magnitude and current potential in an electrochemical cell containing an analyte, which was then used to assess the quantity or recognize targeted compounds for monitoring purposes. The flow of electrons from the oxidation reduction reaction to the adjacent electrode creates electricity and is usually quantified by the current density value. In the case of amphoteric analysis, voltage is held constant that forcing the electron moves to the electrode in order to happen a full cycle of oxidation–reduction reaction [25].

The objective of this analysis is to assess the performance of fabricated WCN as a buffer medium prior to current-volt measurements. An electrolyte scouting assessment was performed to investigate the sensitivity of the sensor from its electron dissociation based on the current generated when voltage is supplied. The electrolyte scouting was measured with I-V measurement, utilizing Keithley 6478 Picoammeter with the supply of current/voltage. The performance assessment was considered on both non-modified AuIDE and surface functionalized AuIDE. Each pH measurement undergoes that scouting starting from solutions pH 1 to 12, followed by a cleaning procedure that is repeated in three times for each pH conditions. The cleaning method was applied to ensure the electrode is electron-free from previous measurements to avoid mixing up with electron dissociation. Both non-modified and functionalized AuIDE chips were performed by using deionized water for measurement in the bare condition. Fig. 5a displays the current generated for non-modified chip. In general, the curvature slope for non-modified with each pH solution was observed and shows small changes for each current generated, starting from the high acidic (pH 1 to 6) to the high alkaline conditions (pH 8 to 12). The difference in amplification can be seen on the, which provides a more detailed curvature current generated. The curvature was noticed to have high sensitivity when it was measured in very high alkaline conditions while it shows small amplification in pH 7. The measurement recorded in pH 10 and pH 12 were to have the highest amplification density current with 9.85 x10^{-11} Ampere and 9.80 x10^{-11} Ampere, respectively. However, the differences between each curve were not significant with all pH levels tested.

Theoretically, when picoammeter voltage was applied, positive charged [H^{+}] ions attract to the cathode while negatively charged [OH^{-}] ions attach to the anode. This process formerly known as electron dissociation and a continuous loop of the system will generate the certain value of current. However, current changes that amplify from synergetic effect contributes to high electron density due to the functionalization of chemical compound. The fabrication onto the surface of the sensor will alter the surface, and thus may modify the degree of dissociation and sensitivity of a sensing system. Thus, the degree of sensitivity is altered due to the electron valency of modified WCN that binds on the AuIDE surface [26,27]. This intrinsic characteristic leads to alteration on the surface of existing AuIDE thus influencing more electron density during electrolyte scouting analysis. It, however, depends on the chemical compound that is attached to AuIDE. In this case, the

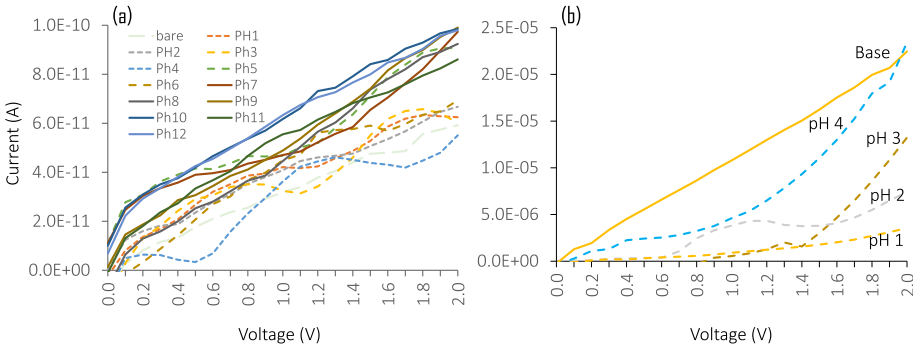

Fig. 5. Electrolyte scouting assessment. a) electrical potential analysis of non-modified chip of AuIDE; b) current generated on WCN modified AuIDE. Tested with pH solutions from 1 to 12.

complexity of WCN led electron valency to give a high degree of dissociation value, thus intensifying the current generated. Ramanathan et al. (2022) who studied electrolyte scouting pointed out that the small amplification of current generated will be one of the best to fit a device [23]. This is due to the fact that small amplification depicted its low degree to increase the current value. Therefore, the device is likely to be robust due to its ability to withstand high values of the voltage applied.

As indicated in Fig. 5b, the current was generated when it applies voltage at different analytes. It was shown that different shapes of current curvature can be observed in comparison to the bare AuIDE. This implies that surface modification of WCN gives different behavior on density current that infers biosensor performance. From the curvature, the density current was amplified higher in the region at a very acidic medium, that is in the range of pH 1 to 4. This has different behavior from Fig. 5a, where no significant differences were seen. This is because the presence of WCN compound alters the surface of AuIDE which gives a higher degree of dissociation in acidic conditions. For example, it was measured that the density current was to be the highest at pH 4 with 2.5 $\times$ 10^{-5} ampere. In further, it means the drift of electron on H^+ ion condition resulting in amplification in comparison to OH^- ion. At this point, the diffusion of current density was recorded to be the highest value then it applied the voltage source. However, when it was performed in neutral pH and alkaline medium, the electric current showed small amplification with almost horizontal lines.

It was worth noting that modified AuIDE during electrolyte scouting analysis, the testing for neutral pH is done after it has applied in very acidic and alkali conditions. This measurement was done check durability of modified AuIDE on its usage in harsh condition at high strength of pH. At highly acidic and alkaline conditions, the buffer contains abundance of [OH^-] and [H^+] ion that may easily be affected to modified AuIDE for measurement at neutral pH. Neutral pH indicates minimal dissociation of electron because at pH 7 involves with very low [OH^-] and [H^+] ion and it is in equal concentration. After AuIDE is applied with very alkali and acidic pH, it was then later applied at pH 7. Analysis shows that the current trend has very low amplification. This indicates insignificant drift of electron, resulted to a very low dissociation of [OH^-] and [H^+]. Insignificant amplification of current trend in pH 7 revealed that the modified AuIDE was performed theoretically because it does not allow any dissociation to take place on both [OH^-] and [H^+] ions. During electrolyte scouting analysis, voltage supply was taken for at least three times to ensure no external factors that could contribute to the analysis. When is it confirmed that is no external factor takes place, extraction of data will then be proceed. Throughout performing electrolyte scouting analysis, it was found that no unusual current trend although the voltage supply attempted to AuIDE in multiple times. Tungsten metal was selected as catalyst precursor due to ability that can withstand high pressure that may induce by physical transformation up to 3640 kPa [28,29]. Furthermore, tungsten is having great material qualities due to high melting point, excellent resistance on corrosion and durable in high temperature [30]. A study by Hidnert and Sweeney (1925) on thermal expansion of tungsten unveil on low coefficient value of tungsten with average range of 4.2–4.8 $\times$ 10^{-6} °C^{-1}, at various temperature range between −100 to 500 °C. This indicates tungsten is an excellent material that resist on material expansion at high low and high temperature [31].

Fig. 6 shows the different values of density current generated at 2 kHz at different pH solutions. Based on the figure, the current density difference gives comparable values in the region between pH 1 to 4 (with more protons) in the range of 7.39 $\times$ 10^{-6} to 2.5 $\times$ 10^{-5} Ampere, whereas the current density difference has relatively low-density current in pH 5 to pH 12 (with low protons), which gives the close ranges. From a micro perspective, the flow of electrons was in abundance to the acidic medium when it is tested with modified WCN. This is because of higher values of current density. Tungsten that is attached to carbon nanoparticles, generally has an oxidation state value of +6. Due to tungsten's unique characteristic, therefore the tungsten formed complex ion and can attach up to six linkages [16]. Furthermore, modifying the electrode surface with two different materials provides a synergetic effect that creates its characters [27]. The binding of W-C coordination alters the electron structure on the commercialized biosensor that promotes its surface performance, which altered the behavior from its existing surface. Apart from that, the anchoring of tungsten onto the defective surface of carbon nanoparticles will aid more electron valence that incorporates in the interstitial of the carbon structure. The phenomenon is known as anchoring. The function of anchoring is the electron valence of carbon and tungsten was to be intercepted, thus there contributing more electron density to the existing carbon nanoparticle. Apart from that, it was noticed there are current densities which measured in negative value. It was known that the conventional electron current movement is from anode to cathode. Therefore, when current density has a negative value, theoretically it is explained that the electron movement is opposite to the conventional electron movement. This concludes electron has more charge density at the cathode, which therefore makes the electron moves from cathode to anode.

Conclusion

The value recorded on modified WCN served as evidence of where nanomaterial binds on AuIDE. Variations of current curvature were observed in amperometry analysis and it gave different current density

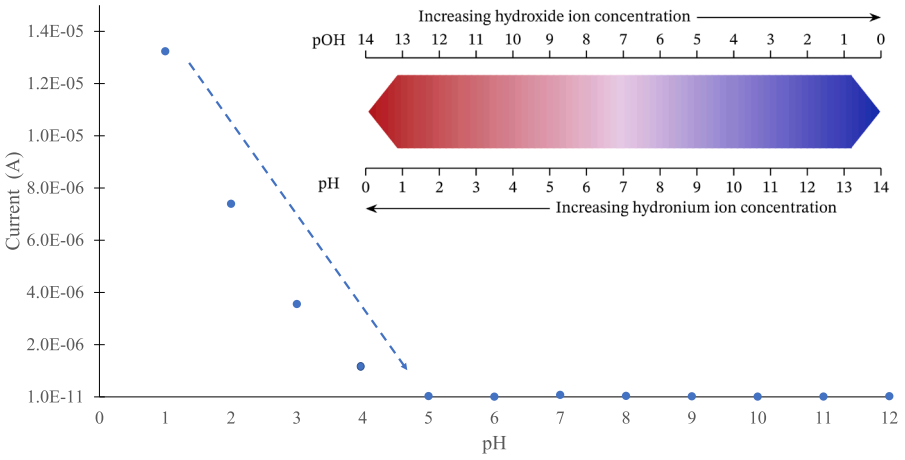

Fig. 6. Electro-determination on WCN modified AuIDE. Clear responses were noticed with changes in protons. Tested by picoammeter power supply to the dual probe station from 0 to 2 V.

values in comparison to commercialized AuIDE. The result from electrolyte scouting shows the dissociation of electrons became greater at pH 4 thus will effect to the electron current density on the electrode terminal. This condition will eventually generate more current flow in the system. The electrolyte scouting for pH 5 to 12, however, gave contradicting results where it showed low amplification of current density. This is by the fact of electron valence on WCN linker together with high [OH–] ion hinders electron movement, thus the electron resists having ion dissociation. Therefore, it gave relatively small amplifications in comparison to pH 4 which shows to give less sensitivity in the presence of [OH^-] ion. The ability of modified WCN to withstand a pH value of 7 shows a very small amplification that is best suited for wide-range applications, especially on biosensors. Furthermore, it also can work in very alkaline conditions which gives insight to be explored for its applicability in extreme conditions. The curvature for modified WCN proved to have the capability to be applied in a wide range of applications that can be useful in further study, especially on its application.

CRediT authorship contribution statement

Hanna Ilyani Zulhaimi: Conceptualization, Methodology, Data curation, Formal analysis, Investigation, Funding acquisition, Investigation, Resources, Validation, Writing – original draft, Writing – review & editing. **Subash C.B. Gopinath:** Data curation, Funding acquisition, Project administration, Resources, Supervision, Visualization, Validation, Writing – original draft, Writing – review & editing. **Farizul Hafiz Kasim:** Data curation, Validation, Visualization, Writing – review & editing. **Periasamy Anbu:** Data curation, Validation, Visualization, Writing – review & editing.

Declaration of Competing Interest

The authors declare that they have no known competing financial interests or personal relationships that could have appeared to influence the work reported in this paper.

Data availability

No data was used for the research described in the article.

Acknowledgement

We would like to thank Yung-Tin Pan, National Tsing Hua University, Taiwan for his support.

References

[1] M. Javaid, A. Haleem, R.P. Singh, S. Rab, R. Suman, Exploring the potential of nanosensors: A brief overview, Sensors Int. 2 (2021), 100130, https://doi.org/10.1016/j.sintl.2021.100130.
[2] C.M. Hussain, R. Keçili, Electrochemical techniques for environmental analysis, Modern Environ. Anal. Tech. Pollutants (2020), https://doi.org/10.1016/b978-0-12-816934-6.00008-4.
[3] M.S. Sumitha, T.S. Xavier, Recent advances in electrochemical biosensors – A brief review, Hybrid Adv. 2 (2023), 100023, https://doi.org/10.1016/j.hybadv.2023.100023.
[4] A. Goel, A. Rastogi, S. Pandey, S. Kulshrestha, S. Goel, An emergent biotechnology hierarchy: Biosensors, Mater. Today:. Proc. (2023), https://doi.org/10.1016/j.matpr.2023.03.363.
[5] M. Vafaiee, M. Vossoughi, R. Mohammadpour, P. Sasanpour, Gold-Plated Electrode with High Scratch Strength for Electrophysiological Recordings, Sci. Rep. 9 (2019) 2985, https://doi.org/10.1038/s41598-019-39138-w.
[6] V. Vojinovic, J.M.S. Cabral, L.P. Fonseca, Real-time bioprocess monitoring, Sens Actuators B Chem. 114 (2006) 1083–1091, https://doi.org/10.1016/j.snb.2005.07.059.
[7] Y. Mie, H. Okabe, C. Mikami, T. Motomura, N. Matsuda, Nanostructured gold thin film electrode derived from surfactant-free gold nanoparticles for enhanced electrocatalysis, Electrochem. Commun. 146 (2023), 107415, https://doi.org/10.1016/j.elecom.2022.107415.
[8] H. Bencherif, F. Meddour, L. Dehimi, G. Faggio, G. Messina, F. Pezzimenti, M. A. Abdi, F.G. della Corte, Improving graphene/4H-SiC/graphene MSM UV photodetector sensitivity using interdigitated electrodes formalism and embedded gold plasmonic nanoparticles, Opt. Laser Technol. 148 (2022), 107683, https://doi.org/10.1016/j.optlastec.2021.107683.
[9] X. Xu, A. Makaraviciute, J. Pettersson, S.-L. Zhang, L. Nyholm, Z. Zhang, Revisiting the factors influencing gold electrodes prepared using cyclic voltammetry, Sens Actuators B Chem. 283 (2019) 146–153, https://doi.org/10.1016/j.snb.2018.12.008.
[10] R. Eivazzadeh Keihan, E. Bahojb Noruzi, E. Chidar, M. Jafari, F. Davoodi, A. Kashtiaray, M. Ghafori Gorab, S. Masoud Hashemi, S. Javanshir, R. Ahangari Cohan, A. Maleki, M. Mahdavi, Applications of carbon-based conductive nanomaterials in biosensors, Chem. Eng. J. 442 (2022), 136183, https://doi.org/10.1016/j.cej.2022.136183.
[11] R. Eivazzadeh-Keihan, E. Bahojb Noruzi, E. Chidar, M. Jafari, F. Davoodi, A. Kashtiaray, M. Ghafori Gorab, S. Masoud Hashemi, S. Javanshir, R. Ahangari Cohan, A. Maleki, M. Mahdavi, Applications of carbon-based conductive nanomaterials in biosensors, Chem. Eng. J. 442 (2022), 136183, https://doi.org/10.1016/j.cej.2022.136183.
[12] B. Lu, L. Liu, J. Wang, Y. Chen, Z. Li, S.C.B. Gopinath, T. Lakshmipriya, Z. Huo, Detection of microRNA-335-5p on an Interdigitated Electrode Surface for Determination of the Severity of Abdominal Aortic Aneurysms, Nanoscale Res. Lett. 15 (2020) 105, https://doi.org/10.1186/s11671-020-03331-y.
[13] H. Li, Y. Li, W. Li, L. Cui, G. Huang, J. Huang, A carbon nanoparticle and DNase I-Assisted amplified fluorescent biosensor for miRNA analysis, Talanta 213 (2020), 120816, https://doi.org/10.1016/j.talanta.2020.120816.
[14] W. Su, P. Yan, X. Wei, X. Zhu, Q. Zhou, Facile one-step synthesis of nitrogen-doped carbon sheets supported tungsten carbide nanoparticles electrocatalyst for hydrogen evolution reaction, Int. J. Hydrogen Energy 45 (2020) 33430–33439, https://doi.org/10.1016/j.ijhydene.2020.09.055.
[15] T.P. Curran, Cyclic and Non-Cyclic Pi Complexes of Tungsten, in: Comprehensive Organometallic Chemistry IV, Elsevier, 2022, pp. 257–377, https://doi.org/10.1016/B978-0-12-820206-7.00108-6.
[16] Z. Chen, W. Gong, Z. Liu, S. Cong, Z. Zheng, Z. Wang, W. Zhang, J. Ma, H. Yu, G. Li, W. Lu, W. Ren, Z. Zhao, Coordination-controlled single-atom tungsten as a non-3d-metal oxygen reduction reaction electrocatalyst with ultrahigh mass activity, Nano Energy 60 (2019) 394–403, https://doi.org/10.1016/j.nanoen.2019.03.045.
[17] C. Paladiya, A. Kiani, Nano structured sensing surface: Significance in sensor fabrication, Sens Actuators B Chem. 268 (2018) 494–511, https://doi.org/10.1016/j.snb.2018.04.085.
[18] H. Liu, T. Zhao, L. Kong, X. Cao, W. Zhu, Y. Huang, M. Bo, Twinning enhanced electrical conductivity and surface activity of nanostructured CuCrO2 gas sensor, Sens Actuators B Chem. 338 (2021), 129845, https://doi.org/10.1016/j.snb.2021.129845.
[19] L. Shen, M.A. Khan, X. Wu, J. Cai, T. Lu, T. Ning, Z. Liu, W. Lu, D. Ye, H. Zhao, J. Zhang, Fe–N–C single-atom nanozymes based sensor array for dual signal selective determination of antioxidants, Biosens. Bioelectron. 205 (2022), 114097, https://doi.org/10.1016/j.bios.2022.114097.
[20] K. Keum, S.S. Cho, J.-W. Jo, S.K. Park, Y.-H. Kim, Mechanically robust textile-based strain and pressure multimodal sensors using metal nanowire/polymer conducting fibers, Iscience. 25 (2022), 104032, https://doi.org/10.1016/j.isci.2022.104032.
[21] K. Nishio, T. Tsuchiya, Electrochromic thin films prepared by sol–gel process, Sol. Energy Mater. Sol. Cells 68 (2001) 279–293, https://doi.org/10.1016/S0927-0248(00)00362-7.
[22] P. Wang, B. Xi, Z. Zhang, M. Huang, J. Feng, S. Xiong, Atomic Tungsten on Graphene with Unique Coordination Enabling Kinetically Boosted Lithium-Sulfur Batteries, Angew. Chem. Int. Ed. 60 (2021) 15563–15571, https://doi.org/10.1002/anie.202104053.
[23] S. Ramanathan, S.C.B. Gopinath, Z.H. Ismail, M.K. Md Arshad, P. Poopalan, Aptasensing nucleocapsid protein on nanodiamond assembled gold interdigitated electrodes for impedimetric SARS-CoV-2 infectious disease assessment, Biosens. Bioelectron. 197 (2022), 113735, https://doi.org/10.1016/j.bios.2021.113735.
[24] H. Krishnan, S.C.B. Gopinath, M.K.M. Arshad, H.Ii Zulhaimi, S. Ramanathan, Molecularly Imprinted Polymer Amalgamation on Narrow-Gapped Archimedean-Spiral Interdigitated Electrodes: Resistance to Electrolyte Fouling in Acidic Medium, Microchimica Acta. 188 (2021) 144, https://doi.org/10.1007/s00604-021-04794-1.
[25] A. Amine, H. Mohammadi, Amperometry, in: Reference Module in Chemistry, Molecular Sciences and Chemical Engineering, Elsevier, 2018, https://doi.org/10.1016/B978-0-12-409547-2.14204-0.
[26] G. Padmalaya, K. Krishna Kumar, P. Senthil Kumar, B.S. Sreeja, S. Bose, A recent advancement on nanomaterials for electrochemical sensing of sulfamethaoxole and its futuristic approach, Chemosphere 290 (2022), 133115, https://doi.org/10.1016/j.chemosphere.2021.133115.
[27] G. Padmalaya, K.H. Vardhan, P.S. Kumar, M.A. Ali, T.-W. Chen, A disposable modified screen-printed electrode using egg white/ZnO rice structured composite as practical tool electrochemical sensor for formaldehyde detection and its comparative electrochemical study with Chitosan/ZnO nanocomposite, Chemosphere 288 (2022), 132560, https://doi.org/10.1016/j.chemosphere.2021.132560.
[28] M.I. McMahon, R.J. Nelmes, High-pressure structures and phase transformations in elemental metals, Chem. Soc. Rev. 35 (2006) 943, https://doi.org/10.1039/b517777b.

[29] N.V. Kozyrev, V.V. Gordeev, Thermodynamic Properties and Equation of State for Tungsten, Crystals (basel). 13 (2023) 1470, https://doi.org/10.3390/cryst13101470.
[30] L. Xu, L. Wang, H. Chen, X. Wang, F. Chen, B. Lyu, W. Hang, W. Zhao, J. Yuan, Effects of pH Values and H2O2 Concentrations on the Chemical Enhanced Shear Dilatancy Polishing of Tungsten, Micromachines (basel). 13 (2022) 762, https://doi.org/10.3390/mi13050762.
[31] P. Hidnert, W.T. Sweeney, Thermal Expansion of Tungsten, Sci. Papers Bureau Standards. 20 (1925) 483–487.